Princetonlaan 6
3584 CB Utrecht
P.O. Box 80015
3508 TA Utrecht
The Netherlands

www.tno.nl

T +31 88 866 42 56
F +31 88 866 44 75

TNO report TNO 2019 R11549 (update 21-05-2021)

Eavor Loop Audit Report

Date 21 may 2021

Author(s) J.D. van Wees

Copy no. 1
No. of copies 1
Number of pages 18
Number of appendices 1
Customer Eavor
Project name Eavor Audit report
Project number 060.42026

Contents

1 Introduction and summary

Eavor has proposed an innovative well design for geothermal energy production, the Eavor Loop™ (Figure 1). The Eavor Loop consists of a closed loop system, in which heat is extracted from the deep subsurface through multi-lateral wells acting as effective heat exchangers.

Eavor has proposed quantitative predictive models for the assessment of the thermal performance and underlying uncertainty of the Eavor loop system (Price et al., 2019).

Eavor has requested in TNO to perform an audit to validate the methods used. Furthermore, Eavor has requested TNO to evaluate the evaluation results of the Eavor Loop demonstration in Canada performed in Q4 2019/Q1 2020 (Price et al., 2020), and later for this update to evaluate the Eavor Loop demonstration for a longer period Q4 2019/Q1 2021. In addition, Eavor has requested TNO to evaluate if the methods proposed can be used in the framework of applications to the Dutch feed-in scheme for geothermal systems (SDE+).

The finding of this audit report are the following:

- The presented models for uniform operating conditions are robust and well capable of predicting the performance of the Eavor Loop
- Analytical approaches appear in excellent agreement with the axisymmetric model results for production temperatures
- Results for varying operating conditions appear correct given the fact that numerically they are based on commercial codes and served as basis for the excellent benchmarked results for uniform operating conditions. It is well known from previous studies on DBHE systems that the type of used axisymmetric models performs well for varying operating conditions
- The 3D numerical models nicely demonstrate the effects of interference and reduced performance when multilaterals are placed at insufficient spacing. Otherwise, the axisymmetric and analytical solutions suffice.
- The Eavor Loop Lite demonstration shows production temperatures which are consistent with analytical model prediction, marked by an excellent correspondence of prediction and observations up to 480 days of running the loop. This close match also demonstrates that the flow rate and inlet temperature is sufficiently stable to use an analytical model for performance assessment.
- For SDE+ applications the analytical approach could be favoured as it provides a transparent, fast and effective basis for assessing and judging the performance of the Eavor Loop. Expectation curves for performance can easily be generated by taking into account uncertainty in relevant parameters, including thermal conductivity and geothermal gradient.

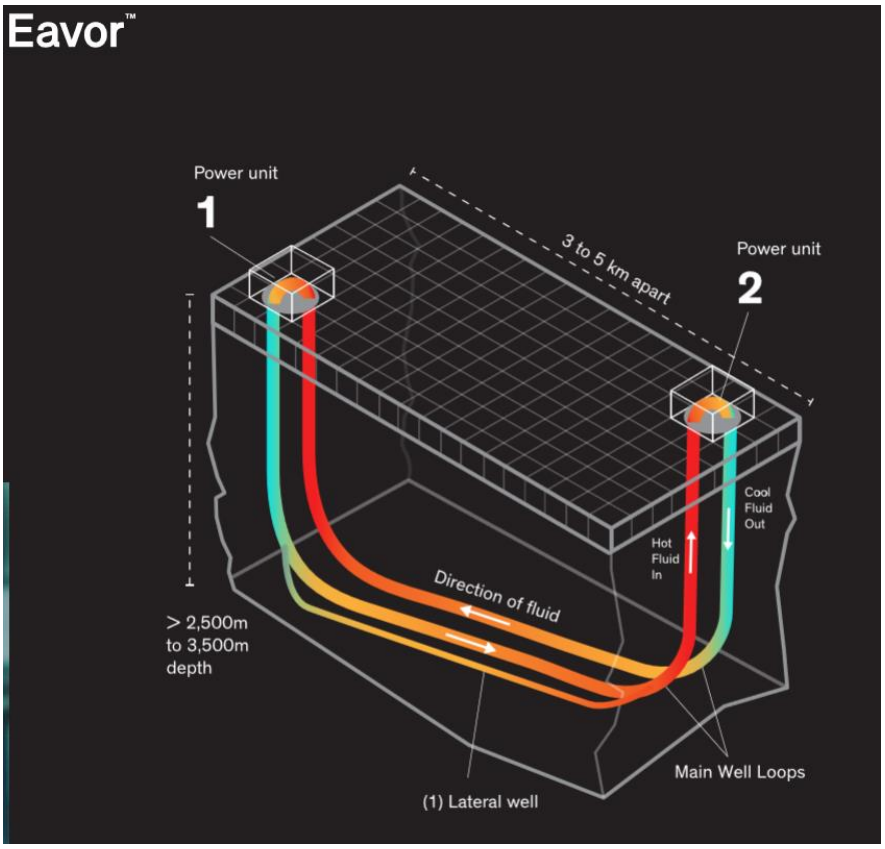

Figure 1 The Eavor Loop™ geothermal production configuration (source Eavor)

2 Model benchmark

Eavor™ has presented three approaches of increasing complexity to predict the thermal output of Eavor-Loop™ projects; using

1. an analytical solution for a single lateral
2. 2-dimensional axisymmetric model for a single lateral
3. 3-dimensional model for multi-laterals

Each of these approaches has been described in detail, and a comparison of the results has been shown for a benchmark case with 1-12 laterals. This benchmark case deals with the (multi-) lateral section (thermal effects of the vertical well paths are neglected) with a length of 5000m, inlet and reservoir temperature, and homogeneous thermal rock properties as listed in Table 1. The flow rate is assumed constant through time running for 25 years.

2.1 Robustness of Analytical and 2-dimensional axisymmetric solution

The results for the production temperature at the end of the lateral show an extremely good match between the analytical solution and the 2D axisymmetric solution reproduced in Figure 2 in this audit. The analytical solution is a so called Line Source Model (Ramey, 1962; Carslaw and Jaeger, 1959; Kutun, 2015):

$$T(r,t) = \frac{q}{2\pi\lambda L} f(t) \qquad \text{(eq. 1)}$$

$$f(t) = \ln(1.4986\sqrt{t_D}) = \frac{1}{2}\left(\ln\left(\frac{4\,k\,t}{r^2}\right) - 0.5772\right)$$

cf. Carlslaw& Jaeger, 1959, Ramey, 1962

$with$

$$\sqrt{t_D} = \sqrt{\frac{k\,t}{r^2}}$$

where $T(r,t)$ is the temperature change relative to ambient temperature at the wall of the well [K], q – heat extracted at the well per unit length (negative [W]), λ – rock conductivity [J K^{-1} m^{-1}], k – rock thermal diffusivity [m^2 s^{-1}], r – radius of well [m], L is length of the well. The derivate of $T(r,t)$ at time *t* [s] is a constant relating temperature change as a function of *f(t):*

$$\frac{1}{k_z} = \frac{dT(r,t)}{dq} = \frac{1}{2\pi\lambda L} f(t) \qquad \text{(eq. 2)}$$

It has been recognized by many authors that equation (1), adopting $f(t) = \ln(1.4986\sqrt{t_D})$ reproduces very well the characteristics of Deep Borehole Heat Exhangers (DBHE) (e.g Kujawa and Nowak, 2000; Van Wees and Lokhorst, 2005; Van Wees et al., 2007; Sapinska-Sliwa et al., 2015). In the analytical approximation for wellbore temperature evolution at time t_s we can write a first order differential equation for $\Theta = T(r, t_s) = (T - T_x)$, where T is temperature in the well and T_x is ambient temperature which can change linearly along the well bore as a function of geothermal gradient (e.g. Kujawa and Nowak, 2000). For a transformed coordinate $x = \frac{X}{L}$, $x \in (0,1)$:

$$\frac{d\Theta}{dx} + k_z^{*}\,\Theta + E^{*} = 0 \qquad \text{(eq. 3)}$$

Where $k_z{}^* = \frac{k_z}{\dot{m}\, c_p}$, $T_x = E^* x + F, E^* = EL$, E – geothermal gradient [K m^{-1}] , F - surface temperature [K], $\dot{m}$ - mass rate [kg s^{-1}], c_p - fluid heat capacity [J kg^{-1} K^{-1}].

The integral solution becomes:

$$\Theta = -\frac{E^*}{k_z{}^*} + \left(\Theta_{x=0} + \frac{E^*}{k_z{}^*}\right) e^{-k_z{}^* x} \quad \text{(eq. 4)}$$

With $\Theta_{x=0}$ is the value of Θ at the entry of the fluid in the well bore. In absence a thermal gradient, eq. 4 matches with the analytical formulation in Price et al., 2019 (their equation 2.18)

$$\frac{T_r - T_{f_{out}}}{T_r - T_{f_{in}}} = exp\left(-\frac{2\pi\lambda L}{\dot{m}c_p \;\; ln\left(1.4986\frac{\sqrt{kt}}{r_w}\right)}\right) \quad \text{(eq. 5)}$$

Parameter	value	unit
reservoir temperature	120	C
length lateral	5000	m
Flow rate per lateral	18	m3/h
Inner diameter lateral	0.156	m
Inlet temperature	60	C
Rhofluid	1000	kg m-3
Cpfluid	4180	J K-1 kg-1
Krock	4	W m-1 K-1
Rhorock	2663	kg m-3
Cprock	1112	J K-1 kg-1

Table 1 benchmark case parameters

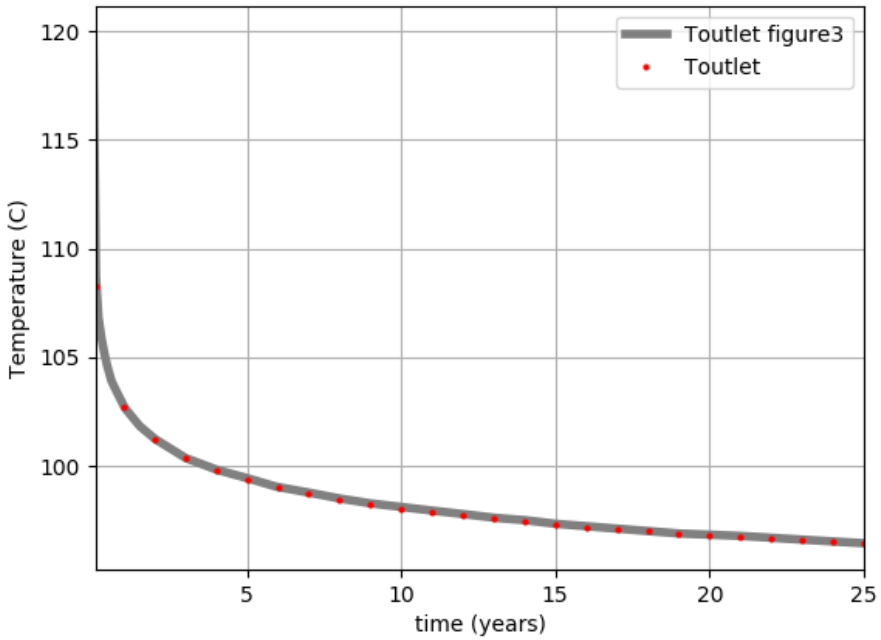

Figure 2 Comparison of 2D numerical axisymmetric model outcome from Price et al., 2019 for a single lateral (from their figure 3) and the analytical model (equation 1, annex 1). Parameters of the model are listed in . See text for explanation.

The results for the benchmark model in the report and reproduced here (Figure 2) clearly show that the borehole geothermal performance can well be predicted with an analytical model when operational conditions are constant over time (i.e. flowrate and inlet temperature), and for homogeneous reservoir conditions.

The 2D numerical models have not been numerically checked in this audit. The approach of Price et al. (2019), using commonly adopted numerical schemes, commercial codes and high mesh resolution. They appear very robust, as is also proven by the close match between numerical and analytical results. This is also consistent with earlier findings of axisymmetric models applied to DBHE studies, including adopted model assumptions such as on effective heat transfer at the well bore interface to the fluids inside the well due to turbulent flow (e.g. Kohl et al., 2002; Lokhorst and Van Wees, 2005). Price et al., (2019) do adopt both the Joule Thomson effect and gravitational potential energy in the numerical solution they use. Ignoring the latter effect in adopting the Joule-Thomson effect in geothermal producton boreholes can lead to an erroneous temperature rise of ca 2 ºC per km (Stauffer et al., 2014).

The comparison shows that analytical solutions suffice very well for the performance assessment, provided operating conditions are relatively uniform in time. If flow rates and inlet temperatures strongly vary over time, the analytical assessment can have limitations (see further in chapter 4).

2.2 3d numerical simulations

The analytical and axisymmetric solutions are adopting infinite radius for cooling, which is fine, as the zone which is affected by cooling is limited and shows not interference with the surface or other laterals. The cooling zone has a cylindrical shape with its axis at the borehole and a radius 0.5 Δx which is a function of time t and depends on the diffusivity, i.e. reproducing equation 2.4.1 from Price et al., 2019:

$$\Delta x = 2\sqrt{\frac{kt}{K}} \qquad \text{(eq.5)}$$

Where *K=1.57* has been set based on best fit with numerical simulation. For the benchmark case, marked by *k=3.65x10*$^{-6}$ m^2 s, this results cooling zones of multi-laterals which do not interfere in the lifetime for the first 10-15 years when $\Delta x = 75\ m$. The thermal effects in 3D simulation (figure 3.) of 12 multilaterals spaced 75 m apart up to 30 years production are indeed minor and in good agreement with the axisymmetric model. The interference for shorter spacing (25 and 50 meter) results in an expected reduction in production temperatures. These models nicely show that the multilaterals need to be spaced sufficiently far from each other, which is well feasible.

Given the relatively low reservoir permeability it is not expected that fluid circulation will be triggered by the cooling of the reservoir surrounding the laterals, in such a way that it can have sufficient impact to alter the thermal calculation results

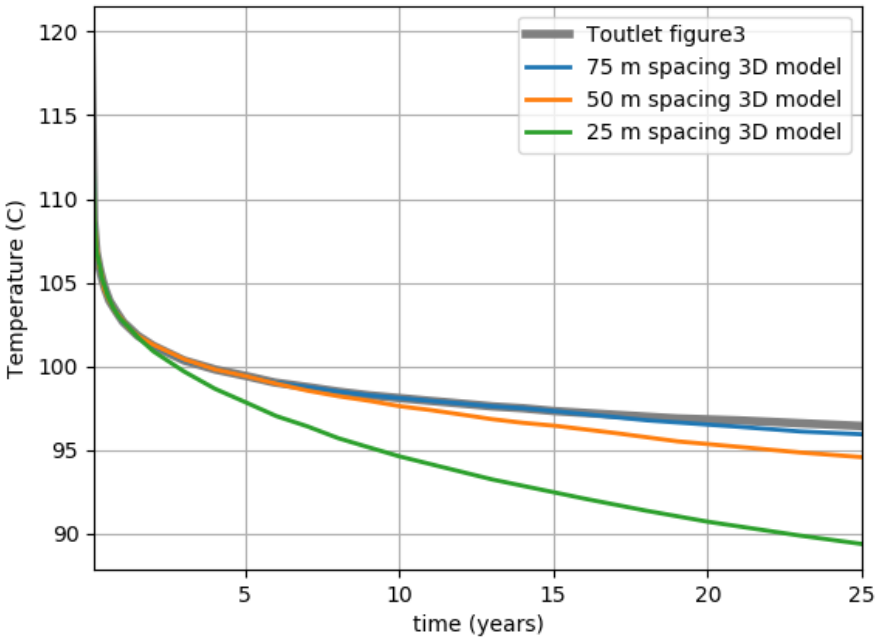

Figure 3 Comparison of 2D (grey) and 3D numerical axisymmetric model outcome from Price et al., 2019 for 12 multilaterals with different spacing and reference solution with a single lateral. See text for explanation.

3 Eavor loop Lite assessment

Price et al., (2019) makes a thermal performance assessment of the Eavor Lite loop, which consist of a pilot in Canada with a one way loop with 2 multi-laterals, with thermal and well parameters of subvertical trajectories (denoted by main) and laterals listed in Table 2.

The subvertical (main) path has an along hole length of ca 2565 m and consists of two sections, which are cased and cemented. The reported inner diameter is interpreted at the interface of the steel casing and the cement as the heat loss is considered negligible in the steel.

Parameter	value	unit
surface temperature	5	C
Main Length (top+bottom section)	2565	m
Main Length (top section)	610	
Lateral length	1920	m
temperature formation	75.95	C
Flow rate	40,000	kg/h
I.D. main (top section)	0.16	m
O.D. main (top section)	0.31	m
I.D. main (bottom section)	0.16	
O.D.main (bottom section)	0.24	
I.D. lateral	0.156	M
# laterals	2	
Tstart	18	C
Cpfluid	4180	J K-1 kg-1
Krock	3.5	W m-1 K-1
Rhorock	2663	kg m-3
Cprock	1110	J K-1 kg-1
Krockmain	2	W m-1 K-1
Krockcement	1.2	W m-1 K-1
Rhorockmain	2240	kg m-3
Cprockmain	1520	J K-1 kg-1

Table 2 Eavor loop lite input parameters

The laterals are approximately 1920 m long.

The axisymmetric model outlet temperature results for constant operating conditions is almost in exact correspondence (< 0.1 C difference) with theTable 1 stepwise analytical solutions for the vertical and horizontal well paths (Figure 4) reproduced in python with annex 2, adopting parameters from Table 2.

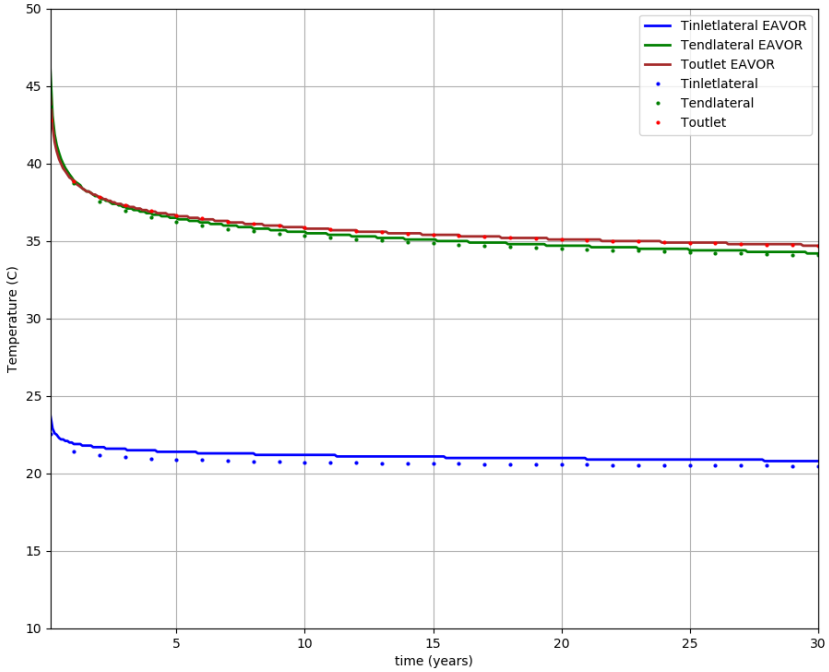

Figure 4 Outlet temperature solution and intermediate temperature solutions and the start and end of the laterals for the Eavor Lite Loop (solid: the EAVOR axisymmetric numerical calculation; dots the piece-wise analytical solution for the Eavor Lite- loop in annex 2).

Please note that the intermediate temperatures at the inlet and outlet of the laterals are slightly different with larger difference (up to ca 1 C) between numerical and analytical solution. These differences are primarily attributed to a) the effect of methalpy in the numerical solution (including Joule-Thompson effect and gravitational potential energy). In addition there may be a minor effect of the longer residence time at relatively high depth and temperatures of the (sub) vertical main in the numerical model, which takes into account the full deviation survey for the numerical calculation

3.1 Sensitivity to cement conductivity contrast, different well bore radius for main.

The axisymmetic numerical solution does not allow for variations in conductivity in radial direction. We did check with the analytical solution what could be the effect of adopting a realistic cement conductivity in between the inner and outer diameter in the borehole. For the subvertical sections the calculation of k_z is (cf. Lokhorst and Van Wees, 2004):

$$\frac{1}{k_z} = \frac{dT(r_i,t)}{dq} = \frac{\frac{\ln\left(\frac{r_o}{r_i}\right)}{\lambda_c} + \frac{f(t)}{\lambda}}{2\pi L} \qquad \text{(eq. 6)}$$

Where r_o and r_i are outer and inner radius of the vertical sections and λ_c is the thermal conductivity of the cement. $f(t)$ is calculated taking $r = r_o$. When the inner and outer diameter are equal eq. 6 reduces to eq. 2.

The results for a cement conductivity of $\lambda_c = 1.2$ do show a very small difference (<<0.1 C) with the reference case presented in Figure 4. Similarly, increase of the inner diameter by 10% of the vertical main has hardly influence on the results.

4 Assesment of Eavor Loop Lite demonstration in Canada Q4 2019/Q1 2020

Eavor has performed Q4 2019/Q1 2020 a demonstration project of the Eavor loop in Canada (Eavor Lite). The setup of the Eavor Loop demonstration is given in Figure 5 and Eavor's detailed evaluation of the results of the demonstration is given in Price et al., 2020. In this section we perform an independent assessment of the demonstration results, in particular in view of thermodynamics analysis.

The geometric setup of the demonstration site and geological conditions are in accordance with section 3, Table 2, except for flow rate, inlet and outlet temperatures and pressures, and adopted thermal conductivities.

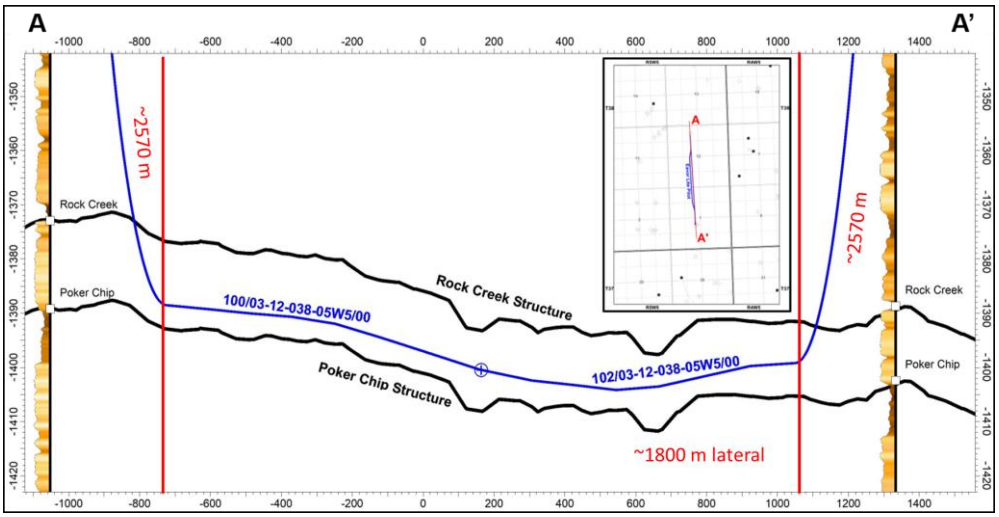

Figure 5 The schematic layout of the Eavor loop Lite demonstration (Price et al., 2020).

Eavor constructed the loop successfully mid 2019 and operated the loop for three months starting December 4 2019, up to March 4 2020. During that time, Eavor measured inlet and outlet temperatures and pressures, flow rate (Figure 6), as well as fluid losses. The latter were minor (average 0.72 m3/day), and are unlikely to affect thermodynamics.

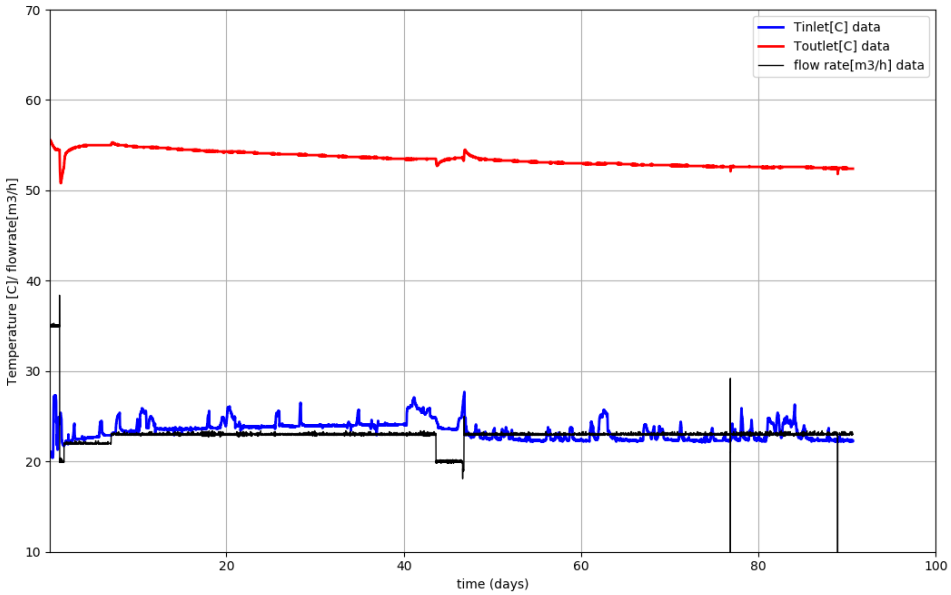

Figure 6 Measured inlet and outlet temperatures, flow rate of the Eavor Lite Loop (data provided by Eavor), starting date is December 4 2019, end date is march 4 2020

4.1 Model Setup

TNO applied its independent analytical model (section 2) to evaluate the Eavor Loop demonstration outcomes. It has been assumed that the analytical model can be used as the flow rate conditions and inlet temperature have been relatively constant (Figure 6). The aim was to determine if the measured outlet temperature given the flow rate and inlet temperature is consistent with the Eavor Lite loop well layout, ambient rock properties and reservoir temperature. The model adopts parameters as listed in Table 2, with modified flow rate, inlet temperature and thermal conductivities in agreement with the yellow marked rows in Table 3. The incorporated rock conductivities have been calibrated by Eavor based on history matching with their numerical performance model, and deviate little (<3%) from pre-spud estimates for the horizontal laterals (Price et al., 2020).

Parameter	Value	Units	Comments
Flow Rate	23.0	m3/h	Average over time span
Inlet Temperature	23.4	ºC	Average over time span
Inlet Pressure	31.0	kPag	Average over time span
Outlet Temperature	52.4	ºC	Last value
Outlet Pressure	304.9	kPag	Last value
Horizontal Thermal Conductivity	4.64	W/mK	History Matched Dec 4 - Feb 2
Vertical Thermal Conductivity	2.25	W/mK	History Matched Dec 4 - Feb 2

Table 3 Parameters in the Eavor Loop Lite demonstration (modified from Price et al., 2020). Those marked in yellow have been adopted in the model.

4.2 Model Results

Figure 7 shows the predicted temperatures of the Eavor Loop Lite demonstration. The predicted outlet temperatures show an excellent match with the observed outlet temperatures after 30 days of operation.

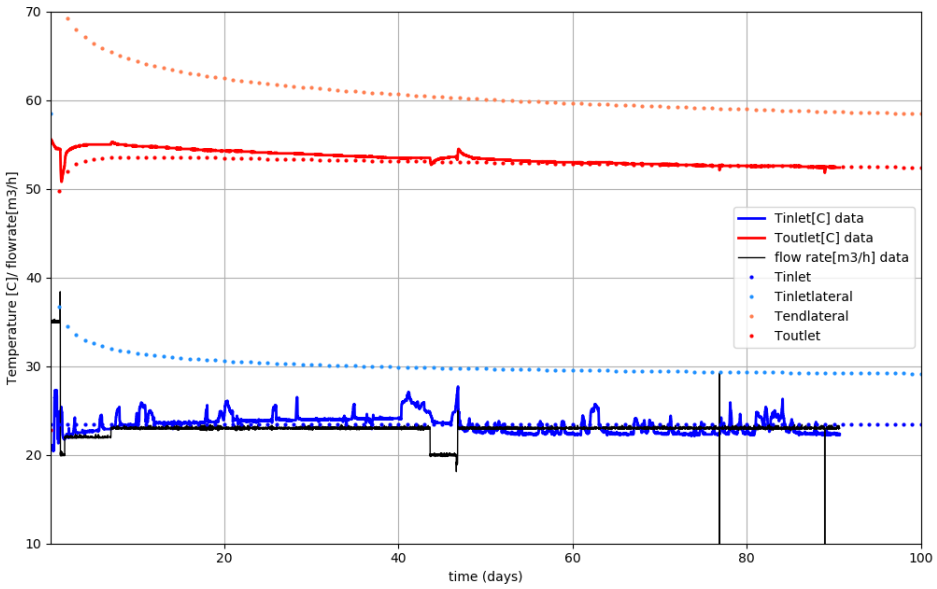

Figure 7 Eavor Loop Lite predicted temperatures (dotted lines) at the subsurface inlet of the lateral segment, end of the lateral, and the outlet temperature.

4.3 Conclusions

The Eavor Loop Lite demonstration shows production temperatures which are consistent with analytical model prediction, marked by an excellent correspondence of prediction and observations after 30 days. This close match also demonstrates that the flow rate and inlet temperature is sufficiently stable to use an analytical model for performance assessment.

5 Update of Assesment of Eavor Loop Lite demonstration in Canada Q4 2019/Q1 2021

The data on the Eavor Loop Lite demonstration have been updated based on data running up to Q1 2021, covering 480 days of operation

5.1 Model Results

Figure 8 shows the predicted temperatures of the Eavor Loop Lite demonstration, with the same parameter settings as in section 4. The long term predicted outlet temperatures show an excellent match with the observed outlet temperatures up to 480 days of operation. The short lived deviations from the long term trend are a consequence of temporary modifications (or arrest) of the flow rate. These short term changes in flow rate cannot be incorporated in the semi-analytical model we use, however we expect that the effects of the short term deviations in flow rate are limited for the long term production temperature. Furthermore, we note that the inlet temperature in the second half of the run time is about 1ºC higher than in the first half. In the semi-analytical model we cannot vary the inlet temperature over time. However, if we run the model with 1ºC higher inlet temperature for the whole duration the effects on the resulting production temperature are minor.

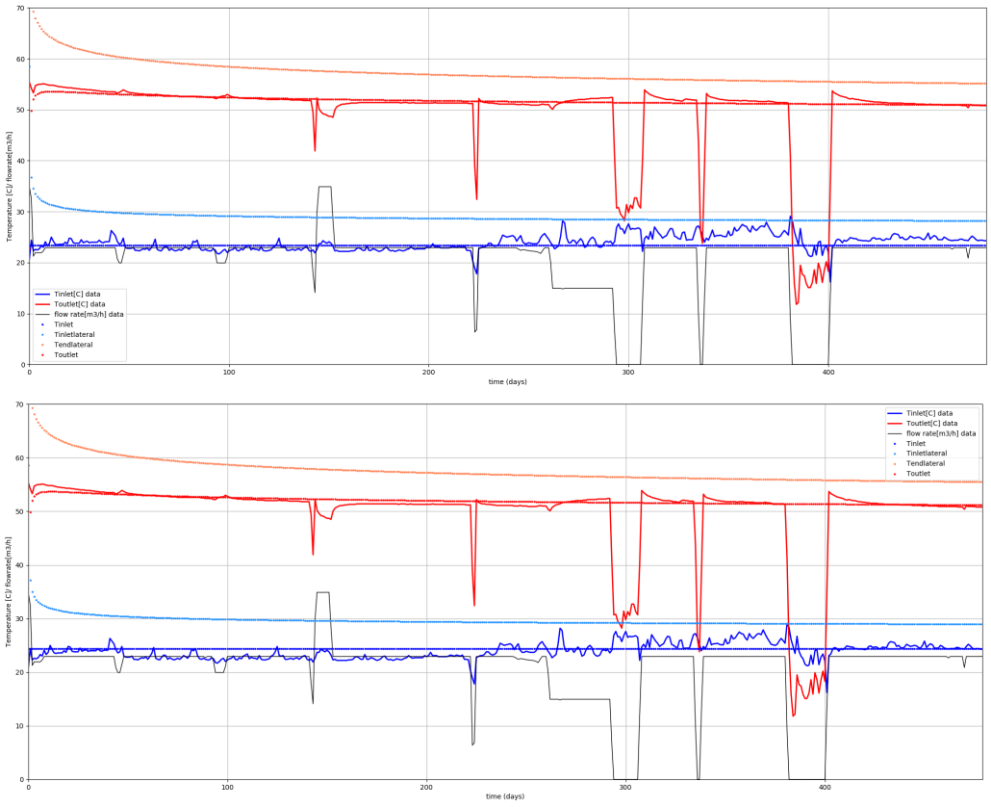

Figure 8 (top) Eavor Loop Lite predicted temperatures (dotted lines) at the subsurface inlet of the lateral segment, end of the lateral, and the outlet temperature (adopting parameter settings from section 4); (bottom) with 1ºC higher inlet temperature.

5.2 Conclusions

The Eavor Loop Lite demonstration shows production temperatures which are consistent with analytical model prediction, marked by a very good agreement of prediction and observations up to 480 days of running the loop.

6 Suitability of methodology for SDE+

The Eavor Loop is a novel geothermal production concept. In this document I assume that RVO can accept the Eavor concept in the 2020 geothermal <4000m category for SDE+, but this needs to be discussed and confirmed from RVO.

If RVO accepts it in the current category, the SDE application requires an expectation curve for the produced geothermal power. For the P50 estimate, I think the approach of Price et al. (2019) for predicting an expectation curve of production temperature at given flow rate is appropriate. The resulting P50 power value is primarily a function of the flowrate [kg/h], thermal properties (which are varied), and I think this may also need to include uncertainty in other subsurface parameters beyond engineering control if this affects the power prediction (e.g. the thermal gradient).

To correctly forecast thermal output of the Eavor loop, thermal conductivity and specific heat of the rock must be correctly estimated. Please note that the adopted values for the benchmark and the Eavor loop lite are specific to that geological formation.

For an estimate of performance for SDE+ the analytical models can be used, provided laterals are sufficiently spaced (see 2.2), and under the assumption that during the SDE load hours the system runs at a flow rate higher or equal that the remainder of the year. The analytical (or axisymmetric) models need to incorporate the effects of heating and cooling of the vertical trajectories of the Eavor loop as these have an effect on the thermal outcome (Figure 4). Interestingly, the effects of the Joule-Thomson and gravitational potential energy effects appear to be of minor influence for the predicted outlet temperatures.

7 Conclusions

The finding of this audit report are the following with respect to the assessment of appropriate predictive models for the hydrothermal performance of the Eavor Loop:

- The presented models for uniform operating conditions are robust and well capable of predicting the performance of the Eavor Loop
- Analytical approaches appear in excellent agreement with the axisymmetric model results for production temperatures
- Results for varying operating conditions appear correct given the fact that numerically they are based on commercial codes and served as basis for the excellent benchmarked results for uniform operating conditions. It is well known from previous studies on DBHE systems that the type of used axisymmetric models performs well for varying operating conditions
- The 3D numerical models nicely demonstrate the effects of interference and reduced performance when multilaterals are placed at insufficient spacing. Otherwise, the axisymmetric and analytical solutions suffice
- The Eavor Loop Lite demonstration shows production temperatures which are consistent with analytical model prediction, marked by an excellent correspondence of prediction and observations up to 480 days of running the loop. This close match also demonstrates that the flow rate and inlet temperature is sufficiently stable to use an analytical model for performance assessment.
- For SDE+ applications the analytical approach could be favoured as it provides a transparent, fast and effective basis for assessing and judging the performance of the Eavor Loop. Expectation curves for performance can easily be generated by taking into account uncertainty in relevant parameters, including thermal conductivity and geothermal gradient.

8 References

Carslaw, H.S., and Jaeger, J.C.: Conduction of Heat in Solids, Oxford at the Clarendon Press, Second Edition (1959), University Press, Oxford, p. 339

Kohl T., Brenni R., and Eugster W.: System performance of a deep borehole heat exchanger, Geothermics, 31, (2002), 687-708

Price, G., Toews, M., Holmes, M., Schwarz, B., Vany, J., 2019. Eavor-Loop™ Thermodynamic Modelling Report. Draft Version received august 28 and commented draft sep 20.

Price, G., Toews, M., Holmes, M., Schwarz, B., Vany, J., 2020. Eavor-Loop™ Demonstration Project Preliminary Technical Report March 9, 2020

Kutun, K., Tureyen, O.I., Satman, A., 2015. Analysis of Wellhead Production Temperature Derivatives. PROCEEDINGS, Fortieth Workshop on Geothermal Reservoir Engineering. Stanford University, Stanford, California, January 26-28, 2015 SGP-TR-204

Kujawa, T., Nowak, W. 2000. Shallow and Deep Vertical Geothermal heat exchangers as low temperature sources for heat pumps. World Geothermal Congress extended abstract.

Lokhorst, A and J.D van Wees, 2005. Technical and economical feasibility of a deep borehole heat exchanger (DBHE) in LTG-01. TNO, NITG 05-068-B0510. Nlog.nl

Ramey, H.J.: Wellbore Heat Transmission, Journal of Petroleum Technology, April 1962, 427-435.

Sapinska-Sliwa, A, and others, 2015. Deep Borehole Heat exchangers – a conceptual review. Proceedings World Geothermal Congress 2015, Melbourne, Australia

Stauffer, P.H., Lewis, K.C., Stein, J.S., Bryan, S. ,Travis, J., Lichtner, P., Zyvoloski, G., 2014. Joule –Thomson Effects on the Flow of Liquid Water. Transp Porous Med. DOI 10.1007/s11242-014-0379-3

Van Wees, J.D., Lokhorst, A., Zoethout, J., 2007. Re-use of E&P-boreholes for geothermal energy production. EAGE conference extended abstract. https://www.tno.nl/media/1662/370beno2.pdf

Annex 1 : python code analytical solution lateral

```
import numpy as np
import matplotlib.pyplot as plt
import os.path

x = np.linspace(0, 25, 26)
x[0] =0.1
tstart = 60
tres = 120
theta0 = tstart-tres
Tinlet = x*0 +tstart


secinyear = 365.25*24*3600 # s

krock = 4.0  # W m-1 K-1
rhorock = 2663 # kg m-3
cprock = 1112 #   J/kg K-1

radius = 0.078 # m
L = 5000 # m
mrate = 18e3  # kg/h
cpfluid = 4180  # J/kg K-1
wdot=   mrate *cpfluid /3600
radius2 = radius*radius

# K formula for C&J
Kfac = 1.4986
overkzK = np.log( Kfac *
np.sqrt((krock/(rhorock*cprock))*x*secinyear/
radius2))/(2*np.pi*krock*L)
kzstar = 1/ (overkzK*wdot)
theta = theta0*np.exp(-kzstar)
Toutlet4 = tres + theta


fig, ax = plt.subplots()

dir = "C:/Users/weesjdamv/review_eavor/"
data = np.loadtxt(os.path.join(dir,'figure3_ana2d.txt'))
line1, = plt.plot(data[:,0], data[:,1], color='grey', linewidth=4,
label='Toutlet figure3')
line2, = ax.plot(x, Toutlet4, "ro",markersize=2,  label='Toutlet')

plt.xlim(0.1,25)

plt.xlabel('time (years)')
plt.ylabel('Temperature (C)')

#plt.semilogx()
plt.grid(True)
ax.legend()
plt.show()
```

Annex 2 : python code analytical Eavor Lite

```
import numpy as np
import matplotlib.pyplot as plt

import os.path

x = np.linspace(0, 30, 31)
x[0] =0.1

tsurface = 5.0 # C
tres = 75.95 # 75.95 # C
depth =   2565.0  #2560.0 # 2365.0 # 2570  # m
depthsurface =  610.0 # surface to first section depth
Estar = tres-tsurface
depthratio = depthsurface/depth
Estar1 = Estar * depthratio
Estar2 = Estar - Estar1
tsection = tsurface + depthratio*Estar
secinyear = 365.25*24*3600

# mass rate of Eavor lite system
mrate = 40e3  # kg/h
# inlet temperature of Eavor system
tstart = 18


# main system
krockmain = 2.0 # W m-1 K-1
krockcement = 1.2  # W m-1 K-1
rhorockmain = 2240 #2240.0 # kg m-3
cprockmain  = 1520.0 #   J/kg K-1

radiussurface =  0.08 # adopt 0.155 to take into account cement
radiussurfaceinner = 0.08 #0.08 # 0.12
radiussurface2 = radiussurface*radiussurface

radiusmain = 0.08 # adopt  0.111   to take into account cement
radiusmain2 = radiusmain*radiusmain
radiusmaininner = 0.08 #0.08 #0.088 # inner radius

# lateral properties
krock = 3.5  # W m-1 K-1
rhorock = 2663.0 # kg m-3
cprock = 1110.0 #   J/kg K-1

radius = 0.078
L = 1920.0 # m
nlateral = 2 # number of laterals
cpfluid = 4180.0 # J/kg K-1
wdot=   mrate *cpfluid /3600.0

Tinlet = x*0 + tstart

Kfacvertical = 1.4986
```

```
# K factor for mains and lateral
Kfac =  Kfacvertical # 1.57 # 1.4986
lsm = np.log(Kfac *
np.sqrt((krockmain/(rhorockmain*cprockmain))*x*secinyear/
radiussurface2))/ krockmain
cement = np.log(radiussurface/radiussurfaceinner)/krockcement
overkzKsurface = (cement + lsm) /(2*np.pi*(depthsurface))
kzstarsurface = 1/ (overkzKsurface *wdot)


lsm = np.log(Kfac *
np.sqrt((krockmain/(rhorockmain*cprockmain))*x*secinyear/
radiusmain2))/ krockmain
cement = np.log(radiusmain/radiusmaininner)/krockcement
overkzKmain = (cement + lsm) /(2*np.pi*(depth-depthsurface))
kzstarmain = 1/ (overkzKmain *wdot)

theta0 = Tinlet - tsurface
theta = -Estar1/kzstarsurface + (theta0+Estar1/kzstarsurface) *
np.exp(-kzstarsurface)
Tsectionbreak = tsurface + theta+Estar1


theta0 = Tsectionbreak - tsection
theta = -Estar2/kzstarmain + (theta0+Estar2/kzstarmain) * np.exp(-
kzstarmain)
Tinletlateral = tsection + theta+Estar2

Kfac =  1.4986 # 1.57 # 1.4986
theta0 = Tinletlateral - tres
radius2 = radius*radius
overkzK = np.log(Kfac *
np.sqrt((krock/(rhorock*cprock))*x*secinyear/
radius2))/(2*np.pi*krock*L)
kzstar = 1/ (overkzK *wdot/nlateral)
theta = theta0*np.exp(-kzstar)
Tendlateral = tres + theta

Kfac =  Kfacvertical # 1.57 # 1.4986
theta0 = Tendlateral - tres
Estar2 = -Estar2
theta = -Estar2/kzstarmain + (theta0+Estar2/kzstarmain) * np.exp(-
kzstarmain)
Tsectionbreak2 = tres + theta+Estar2

theta0 = Tsectionbreak2 - tsection
Estar1 = -Estar1
theta = -Estar1/kzstarsurface + (theta0+Estar1/kzstarsurface) *
np.exp(-kzstarsurface)
Toutlet = tsection + theta+Estar1

fig, ax = plt.subplots()

dir = "C:/Users/weesjdamv/OneDrive -
TNO/wees/geothermie/39.TKIwaylandeavor/review_eavor/"
data =
np.loadtxt(os.path.join(dir,'eavorlite_axicalc_20_nocement.txt'))
```

```
line1, = plt.plot(data[:,0], data[:,1], color='blue', linewidth=2,
label='Tinletlateral EAVOR')
line2, = plt.plot(data[:,0], data[:,2], color='green', linewidth=2,
label='Tendlateral EAVOR')
line3, = plt.plot(data[:,0], data[:,3], color='brown', linewidth=2,
label='Toutlet EAVOR')

# Using set_dashes() to modify dashing of an existing line
line1a, = ax.plot(x, Tinletlateral, "bo",markersize=2,
label='Tinletlateral')
line2a, = ax.plot(x, Tendlateral, "go",markersize=2,
label='Tendlateral')
line3a, = ax.plot(x, Toutlet, "ro",markersize=2,  label='Toutlet')
#line4, = ax.plot(x, Tsectionbreak2, "bo",markersize=2,
label='Tsectionbreak2')



plt.xlim(0.1,30)
plt.ylim(10, 50)

plt.xlabel('time (years)')
plt.ylabel('Temperature (C)')

#plt.semilogx()
plt.grid(True)
ax.legend()
plt.show()
```